IEEE Access
Multidisciplinary | Rapid Review | Open Access Journal

Received October 31, 2018, accepted November 20, 2018, date of publication November 23, 2018,
date of current version December 31, 2018.

Digital Object Identifier 10.1109/ACCESS.2018.2882946

Yanbao: A Mobile App Using the Measurement of Clinical Parameters for Glaucoma Screening

FAN GUO[1,2,3], (Member, IEEE), YUXIANG MAI[1], XIN ZHAO[1,2,3], XUANCHU DUAN[4], ZHUN FAN[5], BEIJI ZOU[1,2,3], AND BIN XIE[1]

[1]School of Information Science and Engineering, Central South University, Changsha 410083, China
[2]Mobile Health Ministry of Education–China Mobile Joint Laboratory, Changsha 410083, China
[3]Hunan Engineering Research Center of Machine Vision and Intelligent Medicine, Central South University, Changsha 410083, China
[4]The Second Xiangya Hospital, Central South University, Changsha 410011, China
[5]Key Laboratory of Digital Signal and Image Processing of Guangdong Province, Shantou University, Shantou 515063, China

Corresponding author: Zhun Fan (zhun_fan@126.com)

This work was supported in part by the National Natural Science Foundation of China under Grant 61502537 and Grant 61573380, in part by the Hunan Provincial Natural Science Foundation of China under Grant 2018JJ3681, in part by the Open Project Fund of the Key Laboratory of Digital Signal and Image Processing of Guangdong Province under Grant 2018GDDSIPL-01, in part by the Mutual Creation Project for teachers and students under Grant 2018gczd022, in part by the 111 Project under Grant B18059, and in part by the Fundamental Research Funds for the Central Universities of Central South University under Grant 2018zzts576.

ABSTRACT Glaucoma is the second leading cause of blindness worldwide, and vision loss from glaucoma cannot be reversed. To remedy this issue, in this paper, a user-friendly mobile App, named Yanbao, is developed. Yanbao App is expected to help users conveniently share high-quality glaucoma screening service by using the proposed glaucoma screening algorithm based on clinical parameters. To the best of our knowledge, it is the first App specially designed for screening glaucoma. The main advantages of our App are: 1) the App has been developed for smartphone, which can be conveniently used at any place and at any time; 2) experiments on both public fundus database and real clinical data demonstrate that the App has good detection and classification accuracy; and 3) users' feedback seems to be quite promising in terms of real-time testing and user experience. Thus, the App could be suitable for glaucoma screening in practice to improve the efficiency of clinicians, balance medical resources, and provide better tiered medical services. The Yanbao App can be available from the website http://url.cn/57tk9jT.

INDEX TERMS Mobile App, clinical parameters, glaucoma screen, cup-to-disc ratio (CDR), neuro-retinal rim (NRR).

I. INTRODUCTION

E-health technologies have been regarded as high potential tools in enhancing healthcare quality, accessibility and delivery. In recent years, the potential of smart technology to provide innovative solutions for disease management has progressively raised high expectations for patients' and healthcare professionals' community [1]. To date, a large number and variety of health-related Apps have been released in the market, ranging from basic apps characterized simply by text message alerts, to sophisticated Apps, helping patients in managing chronic conditions [2]. Some Apps cover a broad spectrum of general medical knowledge, and others can be tailored to specific purposes.

In this paper we present a mobile App specifically designed for the patients with diagnosis of glaucoma, called Yanbao. Glaucoma is the second leading cause of blindness worldwide, as well as the foremost cause of irreversible blindness. Although there is no cure, early detection and treatment can decrease the ratio of blindly. Therefore, an easy-to-use App could be useful for most users. This work addresses this problem by proposing a novel App that allows users to conveniently diagnose glaucoma. The mobile App can be a technological tool useful to help the glaucoma patients manage illness-related issues, thus reducing their burden and let the patients share high-quality screen service at any time and any place. Besides, the mobile App can also improve the efficiency of clinicians, balance medical resources and provide better tiered medical services.

The rest of this paper is organized as follows. In Section II, the related works about the harm and solutions of glaucoma and the related health management applications are reviewed. Section III introduces the design and implementation of

Yanbao App. Section IV describes the internal algorithm of Yanbao App. The experimental studies are given in Section V. Finally, Section VI concludes this paper.

II. RELATED WORK

The most relevant related works fall into the three categories of (a) the harm of glaucoma and its clinical examinations introduced in section II-A, (b) solutions for glaucoma screening discussed in section II-B, and (c) applications that help users to manage their health conditions presented in section II-C.

A. GLAUCOMA AND ITS EXAMINATION

Glaucoma is one of the major leading causes of blindness among eye diseases, predicted to affect around 80 million people by 2020 [3]. Unlike other eye diseases such as cataracts and myopia, vision loss from glaucoma cannot be reversed. Early screening is thus essential for early treatment to preserve vision and maintain life quality. However, many glaucoma patients are not aware of their condition [4]. That is why glaucoma is also called the ''silent theft of sight''. Clinically, there are three examinations practiced to screen glaucoma: intraocular pressure (IOP) measurement, function-based visual field test, and optic nerve head (ONH) assessment [5]. Here, ONH is also called optic disc (OD). IOP is an important risk factor but not specific enough to be an effective detection tool for a great number of glaucoma patients with normal tension. Function-based visual field testing requires specialized perimetric equipment not normally present in primary healthcare clinics. Moreover, the early glaucoma often does not have visual symptoms. ONH or OD assessment is a convenient way to detect glaucoma early, and is currently performed widely by trained glaucoma specialists [6].

Since OD assessment is used as one of the most important measurement indicators for glaucoma screening, our Yanbao App could be useful for allowing users to obtain their related OD information. For OD assessment, segmenting OD is a very important task. Nowadays, many segmentation algorithms have been developed in medical area. For example, Li *et al.* [7] proposed a unified algorithm for automatic glioma segmentation named-UAGS. In UAGS, spatial FCM clustering is first used to estimate the ROI, and then region growing is performed to segment glioma. Chen *et al.* [8] developed a regression convolutional neural network (RegressionCNN) to accurately segment right ventricle from cardiac magnetic resonance images. Gao *et al.* [9] presented an automated framework for detecting lumen and media–adventitia borders in intravascular ultrasound images using an adaptive region-growing method and an unsupervised clustering method. Inspired by the above work, the proposed internal algorithm of Yanbao App also first localized the OD region as the estimated ROI, and then used an improved U-net network to simultaneously segment OD and optic cup (OC) from the ROI for further glaucoma diagnosis.

B. GLAUCOMA SCREENING SOLUTIONS

For large scale screening of glaucoma, color fundus images is suitable due to its cost effectiveness. Therefore, many works have been done toward automated glaucoma detection system by analyzing the input fundus images. For example, Soltani *et al.* [10] designed a new automated diagnostic system to extract the parameters essential for the identification of glaucoma. Soorya *et al.* [11] proposed an automated and robust algorithm for glaucoma diagnosis from fundus images using novel blood vessel tracking and bend point detection. Sousa *et al.* [12] proposed a method that analyzes the texture of the optical disk image region to diagnose glaucoma. Fu *et al.* [5] proposed a Disc-aware Ensemble Network (DENet) for automatic glaucoma screening, which integrates four deep streams on different levels and modules. The multiple levels and modules are beneficial to incorporate the hierarchical representations, while the disc-aware constraint guarantees contextual information from the optic disc region for glaucoma screening. Chai *et al.* [13] proposed to incorporate domain knowledge to construct a two-branch Convolutional Neural Networks (CNN) to learn a classifier for glaucoma diagnosis based on the retinal image. In [14], different classification approaches used so far for detection of glaucoma are provided, and the conclusion that using SVM classifier for the detection of normal and abnormal cases has better performance is also given in this paper.

In conclusion, glaucoma diagnosis usually needs some key clinical parameters and a proper classifier. An easy-to-use App could be useful to allow users to get these clinical parameter values and the probability of having glaucoma.

C. HEALTH MANAGEMENT APPLICATIONS

The mobile Apps have been widely used in medical fields. For instance, Ricci *et al.* [1] developed a mobile App, called AIGkit, specifically designed for adult patients with Pompe disease, with the main aim to help them manage the burden of illness-related factors. Other applications, like the MOST-96120 program was used to determine early cognitive impairment in dementia. The iPad App program provides the sickness scores by letting elderly patients pressing or drawing in the application interface [15]. OphthalDSS is a mobile application tool that helps medical students and primary care professionals make clinical decisions for pink eye disease [16]. Patterson *et al.* [17] designed an application for the diagnosis and prediction of epilepsy, allowing community health workers to screen for diseases like doctors. In [18], a mobile application tool for diagnosing diseases of tongue images is provided. Another iOS program is designed to prevent cardiovascular disease, and the program can predict disease status through the feedback from sensors deployed in the human body [19]. There is also an iOS program to improve the reading of patients with macular degeneration through dynamic text display [20].

Nevertheless, none of these works explicitly provided an easy-to-use mobile application for allowing users to

diagnose glaucoma. The next section introduces a novel App that covers this gap of the literature.

III. DESIGN AND IMPLIMENTATION OF YANBAO APP

As an App tool for assisted screening of glaucoma lesions, Yanbao allows the users to easily obtain and upload their own eye fundus images, and then it will automatically return the test results of key glaucoma indicators and the evaluation of the probability of glaucoma morbidity. Such a tool obeys the usability principle of App software in the development.

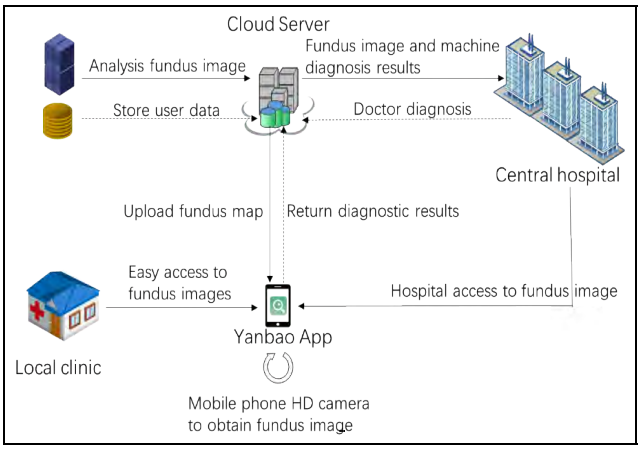

FIGURE 1. Overview of our App application.

Fig. 1 illustrates the functionality of the App application and its operational program. Therefore, users can obtain their high-quality eye fundus images in hospitals and clinics through the professional fundus cameras applied by doctors. Besides, the fundus images can also be obtained through the simple indirect ophthalmoscope provided by users. This App can be employed to upload the fundus images, and will get the glaucoma lesions feedback from the server. In the absence of medical resources and its rapidly increasing demand, this App can greatly alleviate the contradiction by its auxiliary diagnosis.

A. USER INTERFACE

Fig. 2 presents the App's interface for uploading photos. This App allows users to upload personal eye fundus images in two modes. The specific operation is: clicking the "upload photos" button on the home screen can select the mode to upload the fundus image. In this process, obtaining the fundus image through the high-definition camera of the mobile phone needs to be taken with the simple indirect ophthalmoscope, which here refers to a kind of equipment that can clearly observe the human eye fundus image. In addition, the method of obtaining and uploading the fundus images through the album allows the users to apply the relatively high-quality fundus images taken by the ophthalmologist in the hospital. After accomplishing the selection of uploading the fundus image, the system will automatically upload the fundus image by taking the photo album image according to the user's choice.

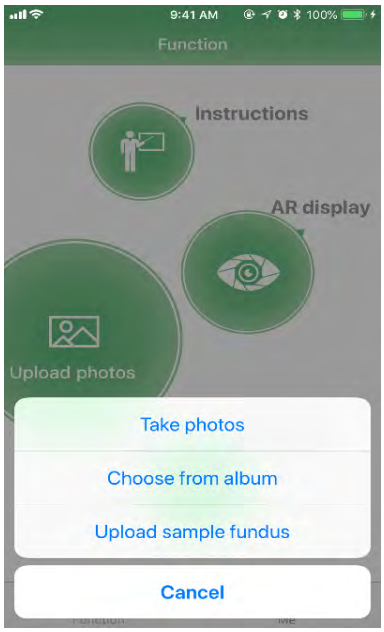

FIGURE 2. Interface of uploading photos for the home screen.

The feedback obtained from this App after uploading the fundus image consists of four parts: CDR analysis, NNR analysis, glaucoma risk prediction, and doctor's diagnosis display. The first three results can be fed back in 10 seconds, and the doctor's diagnosis needs to be interpreted by a professional doctor. When the diagnostic results are obtained, the users can view the results by sliding up and down, or by clicking on the image segmentation image in the diagnostic result interface to check the details of the optic cup and disk image. Fig. 3 shows some examples of detection feedback interface. As can be seen in the figure, the clinical parameters that related to CDR and NNR analysis are shown in Fig. 3(a). These parameters include the area of the OC and OD, vertical and horizontal CDR, the distribution of inferior (I), superior (S), nasal (N) and temporal (T) regions for NNR, etc. Besides, the NNR analysis based on the area, thickness and area ratio with each other are conducted to verify the ISNT rule, as shown in Fig. 3(c). Based on these detected index values, glaucoma risk prediction can be performed, as shown in Fig. 3(b). Since our App is designed to serve doctors as their aided tool, thus doctor's diagnosis display is also provided by the App [see Fig. 3 (b)]. Besides, for the popularization of ophthalmology, the AR effect illustration of the eyeball structure is also provided in our App, as shown in Fig. 3(d). Thus, users can have a better understanding about their own eyes and achieve the self-protection goal through self-awareness. From the above introduction, we can conclude that Yanbao App offers a user-friendly UI for the users.

B. IMPLEMENTATION

Fig. 4 provides the sequence diagram of the diagnosis process. As the sequence diagram shows, the users can select a

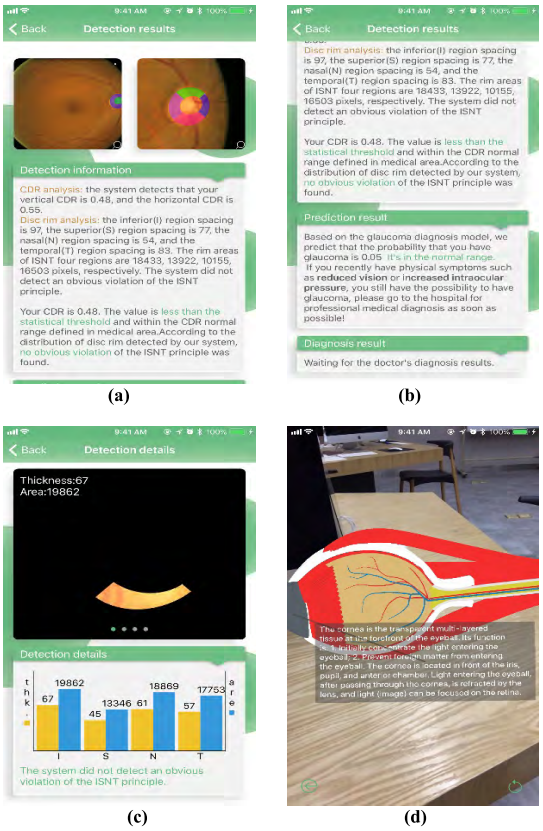

FIGURE 3. Examples of detection feedback interfaces.

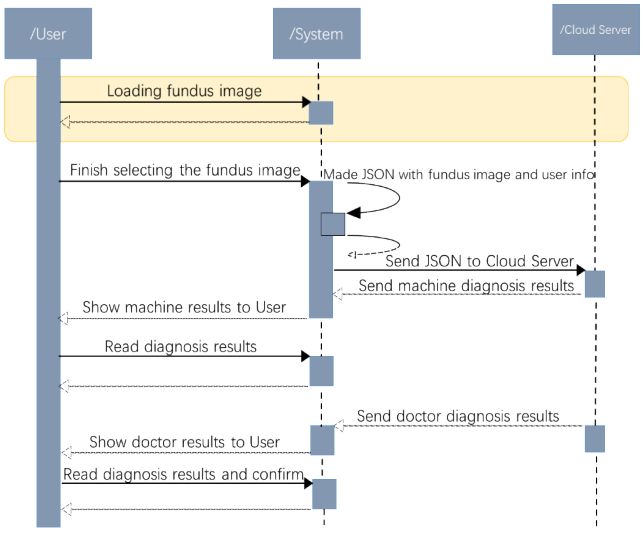

FIGURE 4. Sequence diagram of the diagnosis process.

mode to load the eye fundus image. In this step, the users must select their desired fundus image. For this purpose, the system will first determine whether the image uploaded by the users is a fundus image. If it is a non-fundus image such as a natural image, it will provide a hint that the image is a non-fundus image since the analysis of the image is invalid. In addition, the underexposure or overexposure should be avoided when taking the fundus image and the distortion of the visual disk should be kept as small as possible, which is mainly because the exposure and distortion of the image will have a negative impact on the final analysis effect.

After selecting the fundus image, the system will accept the fundus image and convert it and the user information into JavaScript Object Notation (JSON) file. The converted JSON file will be sent to the cloud server, and the Python script in the cloud server is responsible for receiving and processing the JSON file. JSON is the file format in which the system communicates with the cloud server. The results obtained after processing will be sent back and stored in the database by the database management system (DBMS). Similarly, our App diagnostic information will be sent to the doctor in the same way, and the diagnosis results will be sent to the cloud server after the doctor's diagnosis. In the end, the server will send the final diagnostic information to the users.

Yanbao App requests Web server to send information through Web, especially the POST request. The request comprises the JSON file and the URL of the cloud server managing information and accepting script. When receiving a request, the Python script will perform different operations on JSON files according to different URLs, and update, add, or delete the database. When the request is sent to detect the fundus image, the Python file will process and analyze the image according to the fundus image in JSON, and return the detection result to the mobile device in the form of another JSON file. In this way, the users can detect and update the fundus images.

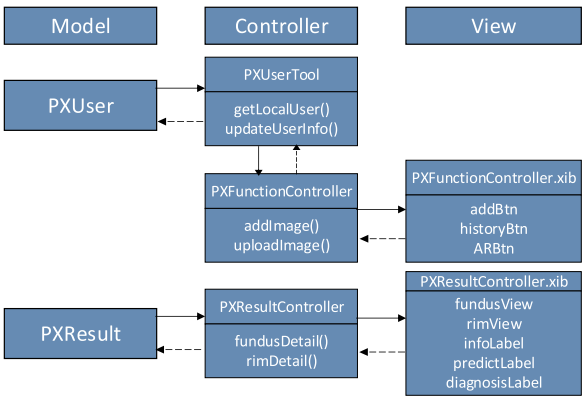

FIGURE 5. Class diagram excerpt of Yanbao app.

The main frame of the Yanbao App is represented by the class diagram structure of Fig. 5, which the whole software is designed by model-view-controller (MVC) architecture pattern. In the architecture, model is responsible for data storage, view is for presentation, and controller is for data processing and linking views and models. When uploading the fundus image for detection, the "PXUserTool" class gets the local user information (such as user ID) modeled on the "PXUser" class and sends it to the

"PXFunctionController" class. Further, the "PXFunction-Controller" loads the fundus image in response to the touch event, and converts the local user information into a JSON file to upload to the cloud server. Moreover, the "PXFunction-Contrller.xib" class is responsible for displaying the interface and getting touch events. PXUserTool is implemented in singleton mode so that there is only one local user. However, the interface file with the same name as Controller and suffix xib is bound to the Controller of the same name so that the events obtained on the user interface can be responded by the controller. In addition, when the detected JSON file is returned, the "PXResultController" class accepts the JSON file, converts the file to the "PXResult" model, and displays the converted model on the "PXResultController.xib" class.

The Yanbao App is developed by the official development framework of iOS applications. The main advantages of iOS application are the high fluency and uniform specification of mobile phone carrier, and the generally equipped high definition camera that is easy to combine with the simple indirect ophthalmoscope to obtain fundus images. Besides, the iOS operating system is a handheld operating system developed by Apple Company of America, which is beautifully designed and easy to operate. In the iOS application development framework, the XIB interface file can be applied to complete the layout of the interface by drag-and-drop, and so on. All these functionalities were relevant for achieving an easy-to-use and intuitive App. Our App runs on iPhone with operation system iOS11 or above, and the App is available to download from Apple's App store (http://url.cn/57tk9jT).

IV. INTERNAL ALGORITHM OF YANBAO APP

The framework of the internal algorithm of Yanbao is presented in Fig. 6, which consists of three main phases: (a) localization and segmentation; (b) measurement of CDR and NRR; and (c) glaucoma risk prediction.

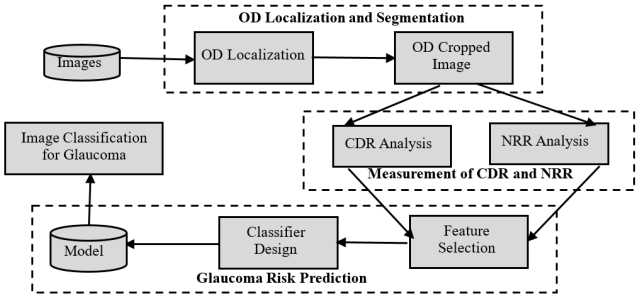

FIGURE 6. Flowchart of the internal algorithm of Yanbao app.

As can be seen in Fig. 6, we first localize and segment the optic disc from an image. Then the measurement of CDR and NRR is performed to deduce the probability of having glaucoma. For example, the higher CDR is corresponding to a higher risk of glaucoma. Finally, the glaucoma risk prediction stage classifies the test image between normal and glaucoma. The subtasks of the block diagram are discussed in the following subsections.

A. LOCALIZATION AND SEGMENTATION

1) OD LOCALIZATION

In the retinal image, the OD and OC occupy small portions, which are hard to segment. To handle this problem, we propose an OD localization algorithm that combines the intensity information with the blood vessels to localize the center of OD through the sliding window. The sub-image cropped from the center of the OD is considered as the ROI region. Thus, the segmentation of OD and OC will be operated on the cropped ROI. Fig. 7 depicts the flowchart of the OD localization algorithm. It can be seen that there are three key steps for localizing the optic disc: Image enhancement and brightest region extraction, blood vessel extraction, and confidence calculation of the sliding window. Following we will discuss the three steps in details.

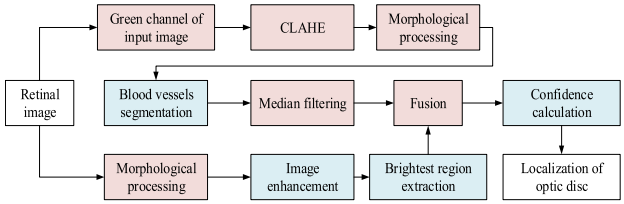

FIGURE 7. Flowchart of the internal algorithm of Yanbao app.

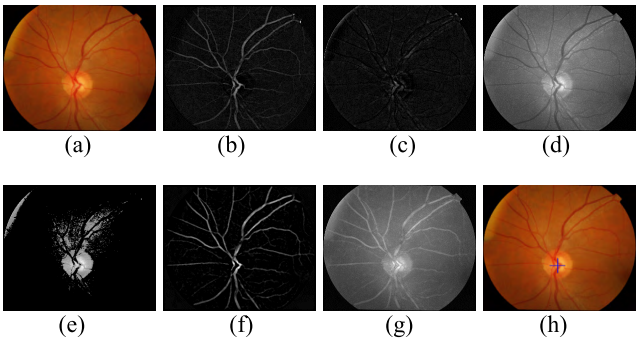

FIGURE 8. Key steps for OD localization. (a) Input retinal image. (b) Bottom-hat transformation result. (c) Top-hat transformation result. (d) Enhanced retinal image by bottom-top-hat transformation. (e) Brightest region of retinal image. (f) Extracted blood vessels. (g) Fusion image which combined enhanced retinal image with the blood vessels. (h) Our OD localization result.

Step 1 (Image Enhancement and Brightest Region Extraction): Due to the various imaging conditions, morphological processing is applied on the input retinal image [see Fig. 8(a)] to enhance the retinal image and to extract brightest pixels from the fundus. Top-hat transformation (G_T) is used to enhance bright objects of interest in a dark background [see Fig. 8(b)], and bottom-hat (G_B) enhances the dark objects of interest in a bright background [see Fig. 8(c)]. Thus, the enhanced gray-level retinal image (F') can be defined as:

$$F' = F + G_T - G_B \tag{1}$$

As can be seen in Fig. 8(d), the region of OD is obviously enhanced, and the contrast of the gray-level retinal image

is enhanced too. Thus, the pixels larger than 6.5 percent of the maximum pixel value are considered to be the candidate pixels of OD, since the OD accounts for brightest region of the retinal image, as shown in Fig. 8(e).

Step 2 (Blood Vessel Extraction): For the blood vessel extraction, Contrast Limited Adaptive Histogram Equalization (CLAHE) is applied to enhance the blood vessel in the green channel of the input retinal image. Then, bottom-top hat transformation is employed to extract blood vessels. Since the intensity of the blood vessels is generally smaller than that of background, the vessels of blood can be extracted by the difference between bottom-hat transformation and top-hat transformation. Besides, to eliminate the salt and pepper noise from the blood vessel segmentation result, median filtering is performed. Thus, the vessel extraction result F_{vessel} can be obtained as shown in Fig. 8(f). This process can be written as:

$$F_{vessel} = G_B - G_T \tag{2}$$

Step 3 (Confidence Calculation of the Sliding Window): To locate the OD fast and effectively, sliding window is employed to scan three different feature maps including brightest region of gray-level retinal image, blood vessels, and the fusion image which combines brightest region and blood vessels, as shown in Fig. 8(g). Let $f(i), f(bv)$ and $f(ibv)$ represent score of each sliding window which is scanned through the three feature maps: intensity map I, blood vessel map bv, and intensity & blood vessel map ibv. In addition, min-max normalization is also applied to the scores of sliding windows in each feature map to normalize the data between 0 and 1. Thus, the final score of each window S is the mean value of $f(i)$, $f(bv)$ and $f(ibv)$.

Finally, the localization of the sliding window with the maximum score will be considered to be the location of OD, as shown in Fig. 8(h).

Once the OD is located, the square region containing OD can be extracted from the retinal image as ROI region. In our work, all the ROI regions have the same size and the size is equal to 1.5 times of the maximum diameter of OD, where the maximum diameter of OD is calculated by the OD mask of retinal images from existing dataset before OD localization. Experiment on test images show that our method can effectively extract the OD inside the ROI region. An illustrative example is shown in Fig. 9. Besides, we evaluate our OD localization method on both ORIGA [21] and DRISHTI-GS1 [22] retinal image datasets, and the statistic results for OD location are shown in Tab. 1. From Tab. 1, one can clearly see that the proposed OD location method achieve high accuracy for the two public databases, and the running speed is relatively fast.

2) OD AND OC SEGMENTATION

Once the OD is located, the segmentation of OD and OC is obtained by our proposed novel deep neural network called U-Net+CP+FL which consists of U-shape convolutional architecture (U-Net) [23], concatenating path (CP) and fusion loss (FL) function, as shown in Fig. 10. As can be seen in the figure, the network includes three components: (i) U-shape deep convolutional neural network architecture, (ii) concatenating path — an additional connection design between encoder layers, and (iii) multi-label output layer with fusion loss function.

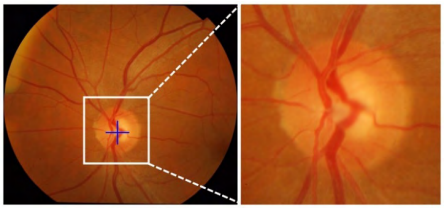

FIGURE 9. OD localization result and cropped ROI region.

TABLE 1. Performance validation of OD localization on different fundus datasets.

Dataset	Image size	Total number	Localization correctly	Accuracy	Time (s)
DRISHTI-GS1	1755×2048	101	101	100%	0.3 s
ORIGA	2048×3072	650	644	99.1%	0.6 s

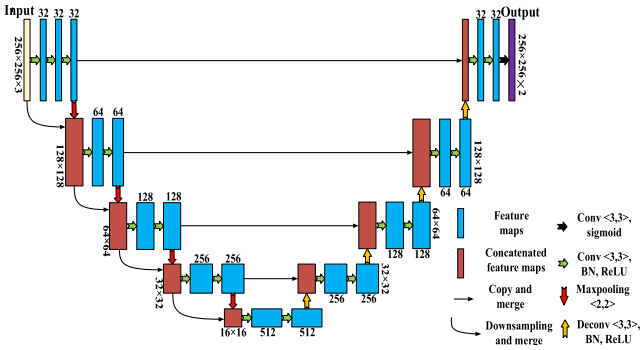

FIGURE 10. Our proposed network architecture.

a: U-SHAPE NETWORK ARCHITECTURE

U-shape network is an effective and powerful fully convolutional neural network for biomedical image segmentation even for small dataset. The network mainly consists of two parts: encoder path and decoder path, and skip connections.

Encoder path is responsible for feature extraction, which consists of convolutional block including batch normalization (BN), ReLU activation and convolutions successively. Maxpooling is employed to reduce the resolution of the feature maps. Decoder path is a reverse process of the encoder path, which is trained to reconstruct the input image resolution. To recover the resolution of the feature maps, deconvolution is employed in the decoder layer which matches pooling layer in the encoder path. Finally, the output at the final decoder layer is fed to a multi-label classifier.

Skip connection is a crucial design in encoder-decoder networks. The skip architecture relays the intermittent feature

maps from encoder layer to the matched decoder layer, which not only helps reconstructing the input image resolution but also overcome the vanishing gradient problem.

b: CONCATENATING PATH

Inspired by Densenet [24], we introduce new connections between encoder layers called concatenating path, which contributes to the feature maps sharing and multi-scale inputs for the encoder path. Along the concatenating path, the input of current layer is consisted of last pooling output and last resized input. Thus, the encoder path receives feature maps not only from the last layer, but also from the input layer and the semantic information from all the previous layers, which equals multi-scale inputs and feature maps sharing. Experimental results show that our proposed network improves the segmentation accuracy.

c: MULTI-LABEL LOSS FUNCTION

OD and OC occupy small parts of retinal image, thus overfitting is prone to happen even trained on the cropped ROI region. In U-NET+CP+FL, we propose combining the weighted binary cross-entropy loss with the dice coefficient loss as the object function to optimize, where the introduction of dice coefficient relives the data imbalance problem effectively. For the proposed network, the output result includes two channels which corresponding to OD and OC segmentation mask respectively, thus multi-label loss means that the pixel belongs to OD or/and OC independently, and this helps to mitigate the data imbalance problem too. The multi-label loss function is described as:

$$L = \lambda_1(L_{CE}^{disc} + L_{dice}^{disc}) + \lambda_2(L_{CE}^{cup} + L_{dice}^{cup}) \tag{3}$$

$$L_{CE} = -\sum_{i=1}^{N} q^i \cdot \log p^i \tag{4}$$

$$L_{dice} = -\sum_{i=1}^{N} \frac{2\left|p^i \cdot q^i\right|}{\left|p^i\right|^2 + \left|q^i\right|^2} \tag{5}$$

where L_{CE}^{disc} and L_{CE}^{cup} represent the cross-entropy loss of OD and OC respectively, L_{dice}^{disc} and L_{dice}^{cup} represent the dice coefficient loss. p^i denotes the predicted probability of pixel i belong to OD in OD segmentation mask or to OC in OC segmentation mask, and q^i denotes the ground truth label for pixel i. λ_1 and λ_2 in Eq. (3) are trade-off weights to decide the contribution of cross-entropy loss and dice coefficient loss. In our work both λ_1 and λ_2 are set to 0.5.

d: TRAINING DETAILS

In our work, the segmentation network is built with Keras which is a high-level neural networks framework and the network is trained with backpropagation algorithm. The ORIGA [21] retinal image dataset is utilized to train and evaluate our proposed network, and 450 retinal images are randomly selected for training, 50 for validation and the remaining 150 retinal images for testing. The training data are the cropped ROI regions which contain the optic disc region and corresponding cropped optic disc and optic cup segmentation masks. During training, we use ADAM method to optimize the network with initial learning rate of 0.0001. All the training images and masks are resized to 256×256. Besides, random flip and rotation, color jitter, random affine transformation are used for training images augmentation, and we train the network with 500 epochs.

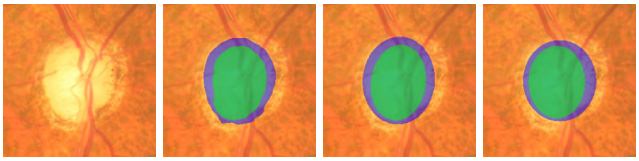

FIGURE 11. CDR calculation result. (a) Original fundus ROI region. (b) Our network segment result. (c) Our ellipse fitting result. (d) Ground truth.

e: POST PROCESSING

An illustrative example for the simultaneous segmentation of OD and OC is shown in Fig. 11(b). To achieve accurate cup-to-disc ratio (CDR) measurement, postprocessing on the segmentation result can mitigate the effects of noise and uneven boundaries. Most isolated points can be eliminated by erosion and dilation operations. Since another distinct feature of OD is its elliptical shape, we then use the least-squares optimization to fit the segmented OD contour with an ellipse, where the contour pixels are extracted by means of a canny edge detector. Finally, the centroid and the long/short-axis length of the OD, which are obtained by ellipse fitting, are used to overlay ellipse on the input image to segment OD of the input retinal image. The same operations are conducted on the OC. Fig. 11(c) shows an example of ellipse fitting result. One can clearly see that both OD and OC boundaries are much smoother and closer to the ground truth after performing ellipse fitting, as shown in Fig. 11(d).

B. MEASUREMENT OF CDR AND NRR

Once OD and OC are simultaneously segmented, some key clinical parameters, such as CDR-related parameters and the ISNT-related parameters can be obtained for glaucoma screening.

For the CDR-related parameters, vertical CDR is calculated by the ratio of the vertical OC diameter (VCD) to the vertical OD diameter (VDD). Other CDR-related parameters include horizontal CDR, optic disc area, optic cup area, CD area ratio, etc.

For the ISNT-related parameters, neuro-retinal rim (NRR) is divided into four different regions named superior NRR region (SNR), inferior NRR region (INR), nasal NRR region (NNR) and temporal NRR region (TNR), according to the distribution of the inferior (I), superior (S), nasal (N), temporal (T) regions in ISNT rule, as shown in Figs. 12(g) to 12(j). Other ISNT-related parameters include INR to disc area ratio, thickness of INR region and area of INR. Besides, INR to OD area ratio and thickness of INR region can be

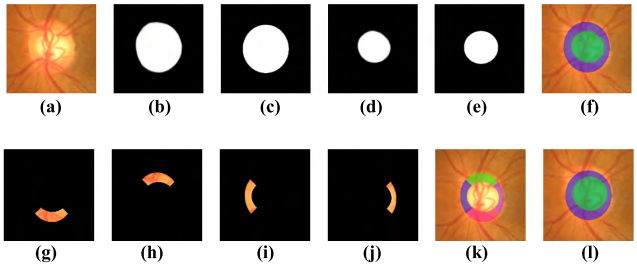

FIGURE 12. First row illustrates the OD and OC segmentation result of fundus ROI region. (a) Original fundus ROI region. (b) OD segmentation of our method. (c) OD segmentation of ground truth. (d) OC segmentation of our method. (e) OD segmentation of ground truth. (f) OD and OC ellipse fitting result of our method. Second row shows the cropped NNR corresponding to I, S, N and T regions. (g) INR. (h) SNR. (i) NNR. (j) TNR. (k) Visualization of NNR on ROI. (l) OD and OC ellipse fitting result of ground truth.

also extracted as clinical parameters to help the glaucoma model judging whether the NRR follows the ISNT rule or not. In summary, 25 features related to segmented OD, OC and NRR analysis are extracted in total. An illustration example of segmented OD, OC and NRR regions are shown in Fig. 12.

C. GLAUCOMA RISK PREDICTION

In order to avoid noisy, redundant or unimportant features to be introduced into the train classifier, an optimal feature set should be selected. Thus, three different feature selection methods are adopted in our work to remove the redundant features.

Specifically, variance analysis is first employed to find features with very low variance which means that those features are constant or nearly distributed around the same value. Then, the correlation analysis is used to measure the correlation between two variables. Variables with strong correlation mean redundant features, and these correlated features make a few contributions to glaucoma classification or even mislead the classifier. Next, feature ranking is used to identity and rank the significant features which are most related to glaucoma classification. Here, features are ranked using the random forest model, and Gini index is also employed to measure the purity of the dataset. Fig. 13 shows the final feature importance rank combined with 10 decision trees for random forest model. Based on the statistic result, 8 features with most importance related to glaucoma classification are selected to train the glaucoma classifier.

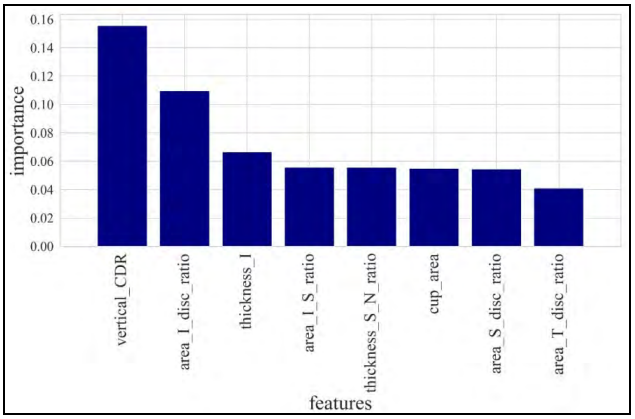

FIGURE 13. Bar graph of the Feature ranking of the selected features. More details about the selected features please see Tab 6 in Appendix.

Note that imbalanced data caused a significant decay in accuracy performance of the classifiers because they are often biased towards the majority class [25], thus in our work synthetic minority over-sampling technique (SMOTE) sampling [26] and class weight method are used to balance the number of features in the normal and abnormal classes. Finally, two candidate classifiers, support vector machine (SVM) or random forest (RF), is used for glaucoma classification. However, RF classifier does not work well under the circumstances for random sampling and inability to data projection, which are not suitable for glaucoma detection. Therefore, SVM classifier is adopted in this work for the automated characterization of the glaucoma and non-glaucoma classes. 10-fold cross-validation is used for glaucoma classification model evaluation.

V. EXPERIMENTAL RESULTS

A. EVALUATION OF PROPOSED ALGORITHM PERFORMANVCE

We measured the proposed internal algorithm from two criteria: (a) segmentation performance, and (b) classification performance. Both performances are evaluated on ORIGA [21] dataset since the dataset provides both OD and OC segmentation mask, CDR values, and glaucoma diagnosis results from ophthalmologist.

1) SEGMENTATION PERFORMANCE

For subjective evaluation, different methods are compared with our proposed U-Net+CP+FL, including U-Net [23] and M-Net with Polar Transformation (M-Net+PT) [27]. The reason why we choose these methods to compare with the proposed U-Net+CP+FL is that U-Net, M-Net+PT and our proposed U-Net+CP+FL are all deep neural network-based method, and the M-Net+PT method is regarded as one of the best OD and OC segmentation methods at present. Fig. 14 shows the results of OD and OC segmentation for different methods. We can clearly see that our proposed U-Net+CP+FL achieves the best segmented boundaries.

Note that all the OD boundaries obtained by different methods are similar. However, the OC segmentation is more a difficult task, and the OC boundary obtained by M-Net+PT is rough and irregular, which will mislead the calculation of CDR. The U-Net achieves a smooth but larger OC. For our results, the boundary of OC is not only smooth but also relatively accurate, thus CDR measurement and glaucoma diagnosis can benefit much from the results.

Quantitative evaluation on OD and OC segmentation are conducted on ORIGA dataset, and the CDR measurement obtained by proposed method is compared to the ophthalmologist. In our experiments, we use the overlap score S [28] and Accuracy ACC [10] respectively to evaluate the

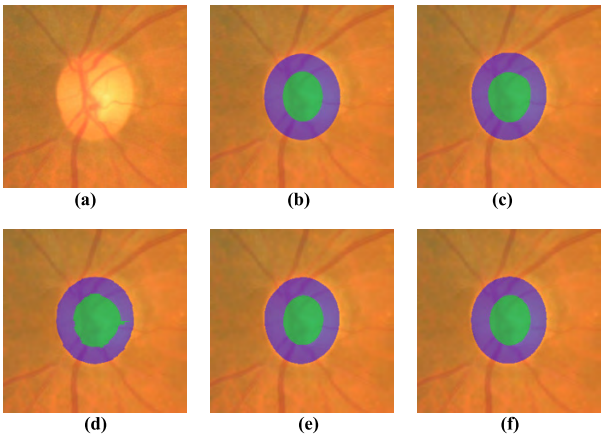

FIGURE 14. Performance comparison of OD and OC Segmentation with different methods. (a) Cropped ROI region. (b) Ground truth. (c) Segmentation result obtained by U-Net. (d) M-Net+PT segmentation result. (e) Proposed method result. (f) Our ellipse fitting result.

segmentation performance. For glaucoma diagnosis, CDR value is an important clinical measurement. Since the ORIGA dataset provides us with the ophthalmologists' CDR values, we can thus evaluate our CDR performance with absolute CDR error, which is defined as $\delta_{CDR} = |CDR_g - CDR_P|$. Here, CDR_g denotes the ground truth from trained clinician, and CDR_P is the CDR calculated by our proposed method.

TABLE 2. Performance comparison of different methods on ORIGA dataset.

Method	S_{disc}	ACC_{disc}	S_{cup}	ACC_{cup}	δ_{CDR}
Superpixel [10]	0.898	0.964	0.736	0.918	0.077
U-Net [18]	0.885	0.959	0.713	0.901	0.102
M-Net+PT [22]	0.929	0.983	0.770	0.930	0.071
U-Net+CP+FL	**0.939**	**0.984**	**0.805**	**0.942**	**0.054**

Besides, several state-of-the-art OD/OC segmentation methods: Superpixel method [29], U-Net [23], and M-Net+PT [27] are adopted to compare with the proposed method. Tab. 2 shows the segmentation comparison results of different methods on ORIGA dataset. Results shows that compared with U-Net, Superpixel achieve better segmentation results both in OD and OC. M-Net+PT which introduces side-output layers and polar transformation makes huge strides in segmentation compared with the original U-Net. However, polar transformation strongly depends on the precise localization of OD, failure of localization would cause the irregular reconstructed segmentation results. In contrast, our network is directly trained on ROI region, which is not sensitive to the result of OD localization. Our proposed U-Net+CP+FL can also achieve best results for all measurements. Besides, smaller error of the calculated CDR δ_{CDR} shows the boundaries obtained by the proposed U-Net+CP+FL method are much finer. Thus, more precise CDR obtained by our method can be used for glaucoma diagnosis.

2) CLASSIFICATION PERFORMANCE

Quantitative evaluation on glaucoma classification performance is conducted on ORIGA dataset [21] and Receiver Operating characteristic (*ROC*) [30] curve is utilized to compare the performance of different glaucoma classifiers. Besides, four evaluation criteria including: *Sensitivity* [30], *Specificity*[30], Accuracy (*ACC*) and area under *ROC* curve (*AUC*) [31] are employed to evaluate the performance of different glaucoma classifiers. The performance of glaucoma classification among different glaucoma classifiers combined with imbalanced data strategies (e.g. SMOTE and class weight) is compared with our work, Tab. 3 shows the comparison result of different classifiers on ORIGA dataset, and the corresponding ROC curves with AUC scores for glaucoma screening is shown in Fig. 15.

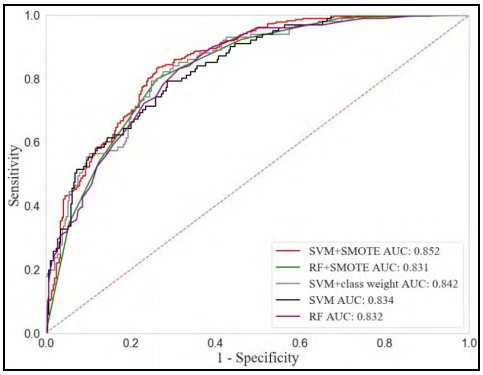

FIGURE 15. ROC curves with AUC scores of different methods for glaucoma classification.

TABLE 3. Performance comparison of different classifiers on ORIGA dataset.

Method	*Sensitivity*	*Specificity*	*ACC*	*AUC*
SVM	0.327	**0.955**	0.641	0.834
SVM+class weight	0.762	0.751	0.757	0.842
SVM+SMOTE	0.751	0.779	0.765	**0.852**
RF	0.396	0.913	0.655	0.832
RF+SMOTE	**0.799**	0.738	**0.769**	0.831

From the Tab. 3 we can conclude that the RF-based glaucoma classifier obtains the best performance on Sensitivity and ACC evaluation criteria. Besides, SVM or RF classifier can obtain very high Specificity while poor Sensitivity which means many glaucoma samples are misclassified as normal when we train the classifiers directly on the raw distribution of the imbalanced dataset, which shows that imbalanced data strategy is very important. Furthermore, comparison between different methods that utilize SMOTE method to address the imbalanced data shows that RF+SMOTE can make 4.8% and 0.4% improvement on Sensitivity and ACC

than SVM+SMOTE respectively. However, SVM+SMOTE achieves best AUC score compared to other methods. Finally, we use RF+SMOTE as our final model to screen glaucoma in our work.

B. CLINICAL SETTING EVALUATION

Since performance on benchmark data is not equal to mobile App environment, we conduct evaluation of Yanbao App in a clinical setting. The evaluation is mainly from three aspects: (a) study design and corresponding statistical results, (b) typical clinical case analysis, and (c) discussion about the advantages and limitations of our Yanbao App.

1) STUDY DESIGN AND STATISTICAL RESULTS

To evaluate the performance of our mobile App, we are working with the second Xiangya Hospital of Central South University to test our Yanbao App. A total of 285 patients with 653 fundus images were collected from the eye clinics of the hospital, all the predictions of our App were compared with ophthalmologists' results. In the study, our diagnosis was based on standard imaging and clinical parameters, and the characteristics of the involved patients with or without glaucoma are illustrated in Tab. 4. For this study, the patient's information, such as gender, age, visiting date, and the diagnosis conclusion given by the ophthalmologist, were collected for comprehensively analyzing the eye disease with the consent of the patients, and other information that involved patients' personal privacy was omitted in the study. From Tab. 4, we can conclude that in clinical setting, the number of patients without glaucoma is much larger than glaucoma patients, and most patients took more than one retinal fundus images at the time of the visit. According to our statistical results, the average age of all patients is 46 years old and the youngest patient is only 4 years old, 90 for the oldest patient. Among the glaucoma patients, the youngest patients are 14 years old, 77 for the oldest patient. Besides, all the collected clinical data has a long span of 7 years, which from October 14, 2010 to March 4, 2017. For the 285 patients, the male patients are slightly more than women. The above collected clinical cases ensure the realness and objectiveness of our performance test.

TABLE 4. Characteristics of the involved patients collected from hospital.

Patient Property	Statistical results
Number of all patients	285
Number of glaucoma patients	86
Number of non-glaucoma patients	199
Number of all retinal fundus images	653
Average Age(range)	46(4-90)
Data time range	2010.10.14-2017.3.4
Sex: Male: Female	107: 98
Eye: Left: Right	261: 392

After further data cleaning, we divide the glaucoma disease into four classes: Primary angle-closure glaucoma, Primary open-angle glaucoma, Secondary glaucoma and Congenital glaucoma. Note that there are different subclasses in secondary glaucoma from our collected data, such as Hemorrhagic glaucoma, Pigmented glaucoma. For the convenience of discussion, all the subclasses are regarded as secondary glaucoma in our study. Fig. 16 shows the comparison results of our App and ophthalmologist's diagnosis for the four main types of glaucoma. One can clearly see that for each type of glaucoma, our App can effectively detect most of the cases and shows a relatively high accuracy. The corresponding glaucoma detection accuracy is shown in Tab. 5. From the table we can deduce that our Yanbao App shows similar performance on both glaucoma and non-glaucoma cases, even the number of glaucoma test cases is much smaller than non-glaucoma cases. For the Secondary glaucoma, there are many subdivisions such as Hemorrhagic glaucoma, Pigmented glaucoma and Malignant glaucoma. Experiment results show that our App can detect most of the subclasses except Malignant glaucoma since the CDR-related and the ISNT-related features are not obvious for Malignant glaucoma. Besides, in our test we also found that patients who failed the test had glaucoma surgery or other eye diseases (e.g. cataracts, etc.), which may increase the detection difficulty and introduce some confusing features. Nevertheless, the vast majority of glaucoma cases can be successfully detected by our App, which shows that the App can not only assist doctors in screening glaucoma, but also help users to assess their own eye health.

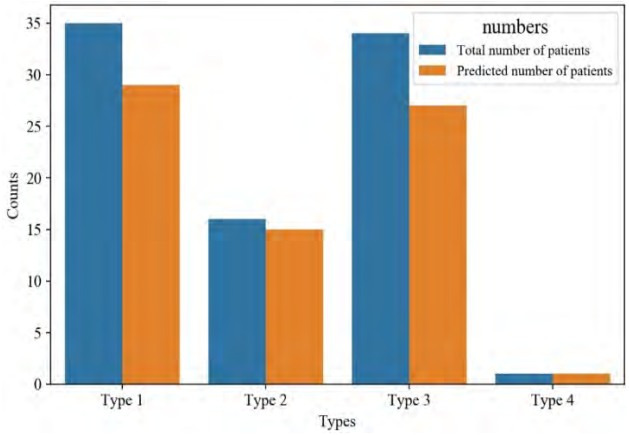

FIGURE 16. The performance of software predictions on different glaucoma types. Type 1: Primary angle-closure glaucoma. Type 2: Primary open-angle glaucoma. Type 3: Secondary glaucoma. Type 4: Congenital glaucoma. Angle-closure glaucoma cases.

TABLE 5. Prediction accuracy for the clinical test data.

Classes	Counts	Predictions	Accuracy
Glaucoma	240	183	0.7625 (Sensitivity)
Non-glaucoma	413	316	0.7651 (Specificity)
All patients	653	499	0.7642

2) CLINICAL CASE ANALYSIS

Clinical case analysis of our App is conducted on 653 retinal fundus images from 285 patients. To verify the robustness and effectiveness of our App, we randomly selected some cases according to the type of glaucoma, such as angle-closure glaucoma, open-angle glaucoma and non-glaucoma. The details on these cases are given below.

a: ANGLE-CLOSURE GLAUCOMA CASES

Two cases of angle-closure glaucoma are shown in Fig. 17(a). The first patient shown in the first row was a female patient who suffered from chronic angle-closure glaucoma. As can be seen in our OD and OC segmentation results of her right eye, the area of the OC has expanded significantly and the peripapillary atrophy appears around the OD. The final prediction for the patient by using our App is glaucoma, which is in consistent with the ophthalmologist's diagnosis. Besides, the patient also has binocular ametropia, whose right eye was in absolute phase, and the left eye in late stage. Another case of angle-closure glaucoma shown in the second row was a female patient who suffered from acute angle-closure glaucoma. From the fundus image of her right eye, we can see that the fundus image is of poor quality and the nasal, nasal-inferior and temporal-inferior regions are hard to recognize. Even in this case, the optic disc and the cup area can be accurately segmented by using Yanbao App. Besides, the patient's eyes also suffered from concurrent cataracts. Although this poses a greater challenge to screening glaucoma, our diagnosis results still seem very promising in this case.

b: OPEN-ANGLE GLAUCOMA CASES

One example of male patient who suffered from binocular open-angle glaucoma and concurrent cataracts is shown in 17(b). One can clearly see that Yanbao App can successfully and accurately segment the enlarged cup area and extract the corresponding features. Finally, the conclusion that the patient has a high-risk of having glaucoma is drawn by our App, which is confirmed by the ophthalmologists' diagnosis result. Another case of open-angle glaucoma is a male patient. From the retinal fundus image of his right eye we can clearly find that the expanded optic cup region is segmented accurately by proposed method and the peripapillary atrophy around the OD is not been misclassified into OD region, which shows the accuracy and robustness of our proposed segmentation network. Besides, the patient also suffered from complicated cataract, optic atrophy and hypertension. Although these complications may interfere with the analysis of Yanbao App, our App still gives a correct prediction in this case with high confidence.

c: NON-GLAUCOMA CASES

Two cases of non-glaucoma are shown in Fig. 17(c). Notice that the two patients were suffering from many other ophthalmology-related diseases. For example, the first female patient suffered from senile cataract which was in the overripe stage with old iridocyclitis and pterygium, while the second female patient has silicone oil eye and complicated cataract. These diseases may cause some problems in fundus imaging and introduce some interference to our glaucoma screening. However, the two patients without glaucoma were diagnosed

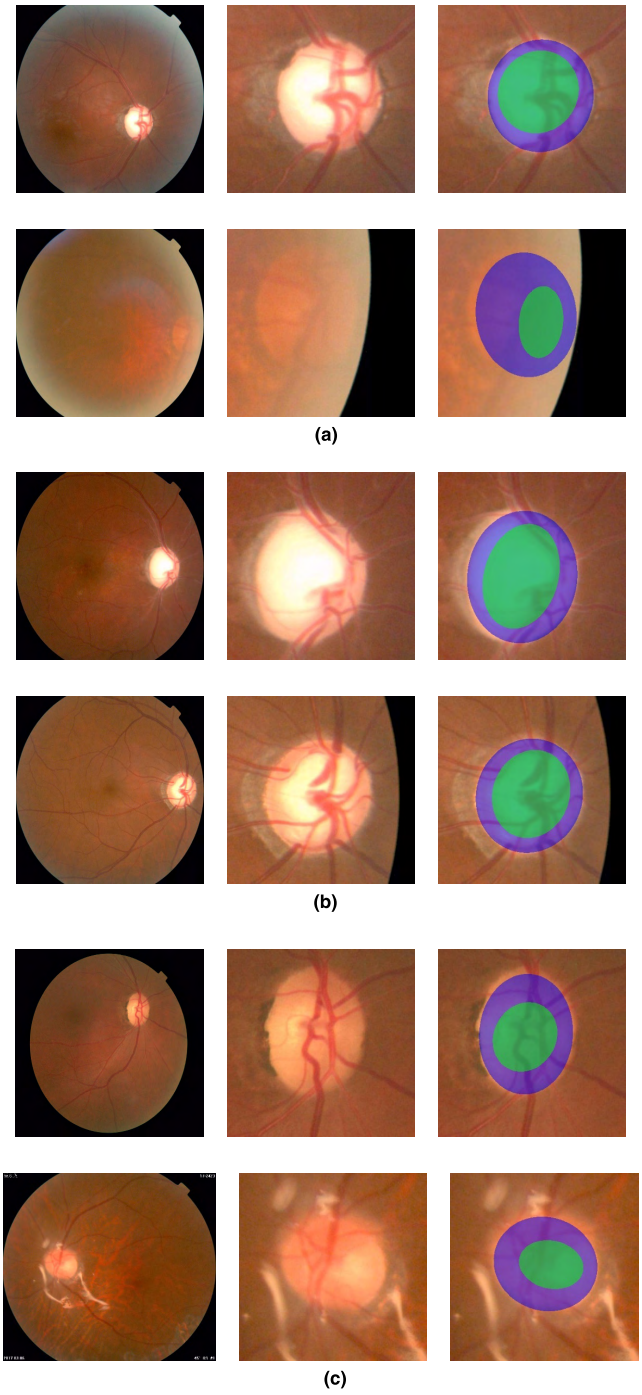

FIGURE 17. Angle-closure glaucoma, open-angle glaucoma and non-glaucoma cases. Each row from left to right: fundus image, estimated ROI and our OD&OC segmentation result, respectively. (a) Angle-closure glaucoma cases. (b) Binocular open-angle glaucoma case. (c) Non-glaucoma cases.

successfully, which demonstrated that our App can deal with such complicated cases very well.

3) DISCUSSION

For clinical setting test on Yanbao App, we identified 285 patients with 653 fundus images for glaucoma classification evaluation. Ophthalmologists' diagnosis conclusion is regarded as a ground truth to evaluate the accuracy of our glaucoma screening App. As can be seen in Tab. 5, of the 240 glaucoma patients, 183 were screened out with an accuracy of 0.7625 (Sensitivity), and 316 of 413 non-glaucoma patients were predicted to be correct, where the accuracy reached 0.7651 (Specificity) which is slightly higher than the Sensitivity. Besides, one can clearly see that the total Accuracy on the fundus images collected from real clinical setting reached 0.7642, which is close to the test performance obtained on public dataset — ORIGA. Thus we can deduce that the proposed algorithm has strong robustness, and Yanbao App can be used as a powerful tool for assisting glaucoma screening.

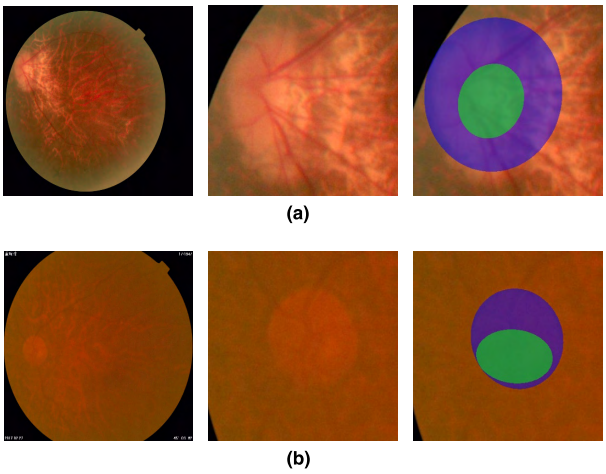

FIGURE 18. Failure cases of glaucoma predictions. From left to right: fundus image, estimated ROI and our OD&OC segmentation result, respectively. (a) A non-glaucoma female case. (b) A non-glaucoma male case.

However, Yanbao App also has some limitations. In our tests, we find that our App may give wrong predictions on some fundus images when the imaging conditions of the fundus images are not very well. These failure situations include: (i) the poor image quality. In this situation, even the ophthalmologist can hardly find the structure and lesions of OD and OC, and (ii) the interference of other eye diseases. These eye diseases may have a bad effect on the final glaucoma prediction. An illustrative example of our failure cases is shown in Fig. 18. In the figure, the case of the first row is a female patient who suffered from the obstruction of lacrimal passage. Another case is a 59 years old male patient who suffered from many diseases, such as complicated cataract, diabetic retinopathy and diabetes. To simultaneously segmenting the OD and OC for the two cases is very hard due to the poor imaging condition or various interference diseases. Although our OC segmentation seem inaccurate since it is hard to find the boundary of OC and the blood vessels in the OD are almost invisible, our proposed segmentation network can still segment the OD precisely in such difficult cases, as shown in Fig. 18. Besides, experimental results show that Yanbao App is able to produce diagnosis results consistent with the ophthalmologists' results in most real clinical cases, which demonstrates that our mobile App has strong robustness and effectiveness and can be used as a powerful tool for glaucoma-assisted screening and diagnosis.

C. EVALUATION OF YANBAO APP PERFORMANCE

To measure the performance of our Yanbao App, three criteria are considered here: (a) real time testing, (b) response time evaluation, and (c) user experience evaluation.

1) REAL TIME TESTING

To test this application, here we use iOS smartphone iPhone 6s Plus as the testing device. Its rear camera reaches 12 megapixels and can take fundus images that meet the clarity requirement of diagnosis if combined with the relevant direct ophthalmoscope. For obtaining accurate experimental results of operational characteristics, we have continuously uploaded multiple fundus images stored in the phone within several minutes and checked the feedback. Figs. 19 and 20 show the usage of CPU and Memory on iPhone 6s Plus while running the App.

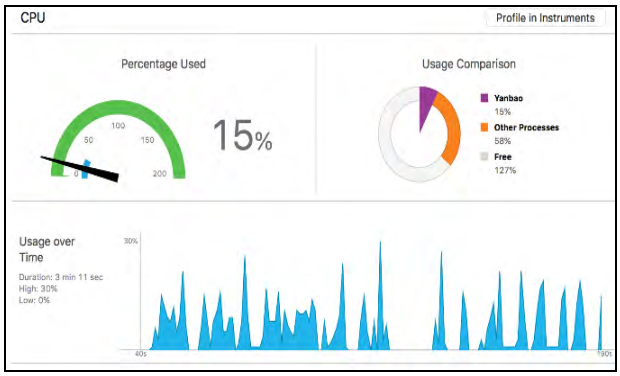

FIGURE 19. Usage of CPU on iPhone 6s Plus while running our App.

As can be seen in these figures, among successive operations, the peak of CPU occupation reaches 30% but just lasts for a short time and exhibits large fluctuations. Then, the peak value of memory consumption is 69.4M and fluctuation is relatively small. This memory consumption is mainly due to multiple images covered in our application as well as in feedback results. In addition, the loading of GUI elements in iOS can also take more memory. But for overall smartphone operation, the memory consumption is less than 4% and in general will not influence the performance of phone for taking up too much CPU and memory resources.

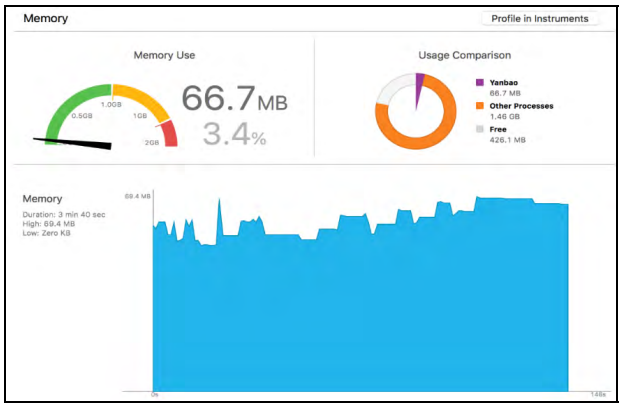

FIGURE 20. Usage of Memory on iPhone 6s Plus while running our App.

2) RESPONSE TIME EVALUATION

Here we have tested the response time of App from uploading file to showing results, which mainly include:

- Convert personal information and fundus images into JSON files.
- Send out POST request and JSON files to cloud server.
- Receive the testing results from server.
- Process the server feedback results and display on the screen.

In order to test the response time more effectively, we carried out experiments of 100 groups and selected fundus images of different specifications in demand of algorithm requirements. Among them, the experimental results of 30 groups have been displayed in Fig. 21.

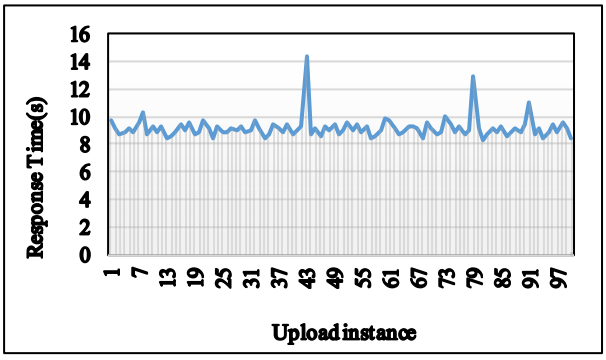

FIGURE 21. The response time of our app.

From the experimental results shown in Fig. 21, we can see that the average response time of 100 group experiments is 9.16s, with standard deviation of 0.78s. One reason for a long response time is that the cloud server has limited computing resources and the processing of fundus images needs some time. Besides, considering there may exist some different delays which depend on the network transition status. Therefore, on the whole, this app system is quite stable, reliable, easy and smooth to operate.

3) USER EXPERIENCE EVALUATION

In order to effectively assess the user experience while using Yanbao App, here we have conducted a series of usability tests and user studies in the form of questionnaires.

a: PARTICIPANT SAMPLES

We have invited 23 people to participate in the survey and they did not know any related information to the APP. The average age of participants is 20.1 years old (age ranges 18-24, standard deviation 1.39). The whole survey group includes 16 male participants (69.5%), 7 female participants (30.4%) and 2 people (8.3%) working or study in the computer science field.

b: STUDY PROCESS

First of all, we introduce the basic ophthalmic knowledge to each participant since the participants cannot use the App without knowing the concept of fundus images, and we also inform them that there already stored some fundus images in the phone. Then, we make a brief introduction to participants about this application and its auxiliary diagnostic function. Note that we don't tell users how to view the diagnostic information in details during this period. That's because we consider that if this application is easy to use, users themselves can easily understand how to use our app functions, and the experimental results also confirm our conclusion. All the participants can complete various functional testing tasks by themselves. Meanwhile, our App also provides an augmented reality (AR) display function. It is an auxiliary function that can place a 3D eyeball model in the scene of real world and make interactions with users. Thus, the AR function can make the App more interactive and interesting, improve user viscosity and popularize the ophthalmology knowledge more validly.

After test completion, participants are required to fill in a questionnaire about this application, which is a System Usability Scale (SUS) [32]. The effectiveness of using SUS to conduct App user test has been verified before, and now SUS is widely used in many systematic evaluation fields. SUS consists of 10 items, which includes alter-natively direct and inverted items. Its rating result is classified as 1-5 levels. (1 refers to "strongly disagree" and 5 refers to "strongly agree"). For the alter-natively direct items, the score is the scale position minus 1. Then for inverted items, the score is 5 minus the scale position. At last, add scores of all the items and get multiply by 2.5 to get the usability score. Since the basic score range of each questionnaire is $0 \sim 40$, after multiply by 2.5, the score for assessment will range from 0 to100.

c: RESEARCH RESULT

All participants have succeeded in completing all the testing tasks under condition of only getting informed of application usage scenarios and functions. Fig. 22 shows more

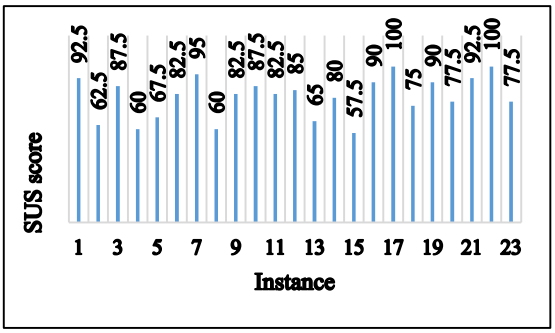

FIGURE 22. The usability scores of all the participants.

details about scores of each participant. As can be seen in the figure, the average score given by all participants is 80.43, which reflects the high usability of this application. Besides, the results also show that the design of user interface is reasonable for users to understand its operation logic.

VI. CONCLUSION

This work has presented a novel mobile App named Yanbao App, which allows users to automatically diagnose glaucoma in real-time. This is useful for reducing glaucoma patients' burden and let them share high-quality screen service at any time and any place. Thus, Yanbao App opens a new channel to improve the efficiency of clinicians, balance medical resources and provide better tiered medical services. The App has been developed for smartphone and has showed a high level of accuracy for both public fundus database and real clinical data. The accuracy mainly due to the internal algorithm of the App, and the users' feedback also seems to be quite promising in most cases. Therefore, our Yanbao App could be suitable for glaucoma screening in practice.

APPENDIX

The selected 8 features with most importance related to glaucoma classification and the corresponding description are shown in Table 6.

TABLE 6. The selected features and corresponding description.

Feature name	Feature description
vertical_CDR	Vertical optic cup-to-disc ratio
area_I_disc_ratio	Area ratio of inferior region in neuroretinal rim to optic disc
thickness_I	Thickness of inferior region in neuroretinal rim
area_I_S_ratio	Area ratio of inferior region to superior region in neuroretinal rim
thickness_S_N_ratio	Thickness ratio of superior region to nasal region
cup_area	Area of optic cup
area_S_disc_ratio	Area ratio of superior region in neuroretinal rim to optic disc
area_T_disc_ratio	Area ratio of temporal region in neuroretinal rim to optic disc

ACKNOWLEDGMENT

The authors would like to thank the staff from the Second Xiangya Hospital of Central South University of China who provided the real clinical data and consented to participate and publish study findings, especially Professor Xuanchu Duan and Dr. Pingbo Ouyang. They would want to thank all the members of Intelligent Medical Imaging Research Group (iMED), especially Professor Jiang Liu who provided the ORIGA dataset for us. And They would also want to thank the team of Professor Shuo Li who gave us many valuable suggestions during our research.

REFERENCES

[1] G. Ricci *et al.*, "A mobile app for patients with Pompe disease and its possible clinical applications," *Neuromuscular Disorders*, vol. 28, no. 6, pp. 471–475, 2018.
[2] M. N. K. Boulos and N. M. Al-Shorbaji, "On the Internet of Things, smart cities and the WHO healthy cities," *Int. J. Health Geograph.*, vol. 13, no. 1, pp. 1–10 2014.
[3] Y.-C. Tham, X. Li, T. Y. Wong, H. A. Quigley, T. Aung, and C.-Y. Cheng, "Global prevalence of glaucoma and projections of glaucoma burden through 2040: A systematic review and meta-analysis," *Ophthalmology*, vol. 121, no. 11, pp. 2081–2090, 2014.
[4] S. Y. Shen *et al.*, "The prevalence and types of glaucoma in malay people: The singapore malay eye study," *Invest. Ophthalmol. Vis. Sci.*, vol. 49, no. 9, pp. 3846–3851, 2008.
[5] H. Fu *et al.*, "Disc-aware ensemble network for glaucoma screening from fundus image," *IEEE Trans. Med. Imag.*, vol. 37, no. 11, pp. 2493–2501, Nov. 2018, doi: 10.1109/TMI.2018.2837012.
[6] H. Fu *et al.*, "Segmentation and quantification for angle-closure glaucoma assessment in anterior segment OCT," *IEEE Trans. Med. Imag.*, vol. 36, no. 9, pp. 1930–1938, Sep. 2017.
[7] Q. Li *et al.*, "Glioma segmentation with a unified algorithm in multimodal MRI images," *IEEE Access*, vol. 6, pp. 9543–9553, 2018.
[8] J. Chen, H. Zhang, W. Zhang, X. Du, Y. Zhang, and S. Li, "Correlated regression feature learning for automated right ventricle segmentation," *IEEE J. Transl. Eng. Health Med.*, vol. 6, 2018, Art. no. 1800610.
[9] Z. Gao *et al.*, "Automated framework for detecting lumen and media–adventitia borders in intravascular ultrasound images," *Ultrasound Med. Biol.*, vol. 41, no. 7, pp. 2001–2021, 2015.
[10] A. Soltania, T. Battikh, I. Jabri, and N. Lakhoua, "A new expert system based on fuzzy logic and image processing algorithms for early glaucoma diagnosis," *Biomed. Signal Process. Control*, vol. 40, pp. 366–377, Feb. 2018.
[11] M. Soorya, A. Issac, and M. K. Dutta, "An automated and robust image processing algorithm for glaucoma diagnosis from fundus images using novel blood vessel tracking and bend point detection," *Int. J. Med. Inform.*, vol. 110, pp. 52–70, Feb. 2018.
[12] J. A. de Sousa, A. C. de Paiva, J. D. S. de Almeida, A. C. Silva, G. Braz, Jr., and M. Gattass, "Texture based on geostatistic for glaucoma diagnosis from fundus eye image," *Multimedia Tools Appl.*, vol. 76, no. 18, pp. 19173–19190, 2017.
[13] Y. Chai, L. He, Q. Mei, H. Liu, and L. Xu, "Deep learning through two-branch convolutional neuron network for glaucoma diagnosis," in *Proc. Int. Conf. Smart Health*, 2017, pp. 191–201.
[14] N. Thakur and M. Juneja, "Survey of classification approaches for glaucoma diagnosis from retinal images," in *Advanced Computing and Communication Technologies*, vol. 562. Cham, Switzerland: Springer, 2017, pp. 91–99.
[15] M. Clionsky and E. Clionsky, "The MOST-96120 iPad app improves PCP Alzheimer's disease screening," *Alzheimers Dementia, J. Alzheimer's Assoc.*, vol. 8, no. 4, pp. S755–S756, 2012.
[16] M. M. López, M. M. Lôpez, I. de la Torre Díez, J. C. P. Jimeno, and M. López-Coronado, "A mobile decision support system for red eye diseases diagnosis: Experience with medical students," *J. Med. Syst.*, vol. 4, no. 6, pp. 151-1–151-10, 2016.
[17] V. Patterson, S. Samant, M. B. Singh, P. Jain, V. Agavane, and Y. Jain, "Diagnosis of epileptic seizures by community health workers using a mobile app: A comparison with physicians and a neurologist," *Seizure*, vol. 55, no. 4, pp. 4–8, 2018.

[18] R. Kanawong, T. Obafemi-Ajayi, D. Liu, M. Zhang, D. Xu, and Y. Duan, "Tongue image analysis and its mobile app development for health diagnosis," in *Translational Informatics in Smart Healthcare* (Advances in Experimental Medicine and Biology). Cham, Switzerland: Springer, 2017.
[19] L. Moreno-Alsasua, B. Garcia-Zapirain, J. D. Rodrigo-Carbonero, I. O. Ruiz, S. Hamrioui, and I. de la Torre Díez, "Primary prevention of asymptomatic cardiovascular disease using physiological sensors connected to an iOS app," *J. Med. Syst.*, vol. 41, no. 12, pp. 191-1–191-9, 2017.
[20] R. Walker, "An iPad app as a low-vision aid for people with macular disease," *Brit. J. Ophthalmol.*, vol. 97, no. 1, pp. 110–112, 2012.
[21] Z. Zhang *et al.*, "ORIGA^{-light}: An online retinal fundus image database for glaucoma analysis and research," in *Proc. Annu. Int. Conf. IEEE Eng. Med. Biol.*, Aug./Sep. 2010, pp. 3065–3068.
[22] J. Sivaswamy, S. R. Krishnadas, A. Chakravarty, and . D. Joshi, "A comprehensive retinal image dataset for the assessment of glaucoma from the optic nerve head analysis," *JSM Biomed. Imag. Data Papers*, vol. 2, no. 1, pp. 1004-1–1004-7, 2015.
[23] O. Ronneberger, P. Fischer, and T. Brox, "U-net: Convolutional networks for biomedical image segmentation," in *Proc. Int. Conf. Med. Image Comput. Comput.-Assist. Intervent.*, 2015, pp. 234–241.
[24] G. Huang, Z. Liu, L. van der Maaten, and K. Q. Weinberger, "Densely connected convolutional networks," in *Proc. IEEE Conf. Comput. Vis. Pattern Recognit.*, Jul. 2017, pp. 2261–2269.
[25] J. Liu, Q. Hu, and D. Yu, "A comparative study on rough set based class imbalance learning," *Knowl.-Based Syst.*, vol. 21, no. 8, pp. 753–763, 2008.
[26] N. V. Chawla, K. W. Bowyer, L. O. Hall, and W. P. Kegelmeyer, "SMOTE: Synthetic minority over-sampling technique," *J. Artif. Intell. Res.*, vol. 16, no. 1, pp. 321–357, 2002.
[27] H. Fu, J. Cheng, Y. Xu, D. W. K. Wong, J. Liu, and X. Cao, "Joint optic disc and cup segmentation based on multi-label deep network and polar transformation," *IEEE Trans. Med. Imag.*, vol. 37, no. 7, pp. 1597–1605, Jul. 2018.
[28] M. Niemeijer, M. D. Abràmoff, and B. van Ginneken, "Segmentation of the optic disc, macula and vascular arch in fundus photographs," *IEEE Trans. Med. Imag.*, vol. 26, no. 1, pp. 116–127, Jan. 2007.
[29] J. Cheng *et al.*, "Superpixel classification based optic disc and optic cup segmentation for glaucoma screening," *IEEE Trans. Med. Imag.*, vol. 32, no. 6, pp. 1019–1032, Jun. 2013.
[30] A. G. Lalkhen and A. McCluskey, "Clinical tests: Sensitivity and specificity," *Continuing Edu. Anaesthesia, Critical Care Pain*, vol. 8, no. 6, pp. 221–223, Dec. 2008.
[31] J. Huang and C. X. Ling, "Using AUC and accuracy in evaluating learning algorithms," *IEEE Trans. Knowl. Data Eng.*, vol. 17, no. 3, pp. 299–310, Mar. 2005.
[32] F. González-Landero, I. García-Magariño, R. Lacuesta, and J. Lloret, "PriorityNet app: A mobile application for establishing priorities in the context of 5G ultra-dense networks," *IEEE Access*, vol. 6, pp. 14141–14150, 2018.

FAN GUO (M'15) received the B.S. degree in computer science and technology and the M.S. and Ph.D. degrees in computer application technology from Central South University (CSU), Changsha, China, in 2005, 2008, and 2012, respectively. She is currently an Associate Professor with the School of Information Science and Engineering, CSU. Her main research interests include image processing, computer vision, and pattern recognition.

YUXIANG MAI is currently pursuing the B.S. degree in computer science and technology with the School of Information Science and Engineering, Central South University, Changsha, China. His research interests include digital image processing, computer vision, and iOS mobile application development.

XIN ZHAO is currently pursuing the M.S. degree with the Mobile Health Ministry of Education–China Mobile Joint Laboratory, School of Information Science and Engineering, Central South University, Changsha, China. His research interests include digital image processing, computer vision, and machine learning.

XUANCHU DUAN has also served as the Chief Ophthalmologist, the Deputy Director of ophthalmology, and the Director of glaucoma specialist at The Second Xiangya Hospital, Central South University. He is currently a Professor of ophthalmology and a Doctoral Supervisor with Central South University. He has published 110 papers and nearly 30 SCI-indexed papers. He has also authored more than 10 books.

ZHUN FAN received the B.S. and M.S degrees from the Huazhong University of Science and Technology, China, in 1995 and 2000, respectively, and the Ph.D. degree from Michigan State University, USA, in 2004. He is currently a Professor with the Department of Electronic and Information Engineering, Shantou University, where he has also served as the Dean of the Key Laboratory of Digital Signal and Image Processing of Guangdong Province. His research focus is on computer vision, machine learning, and artificial intelligence.

BEIJI ZOU received the B.S. degree from Zhejiang University, Hangzhou, China, in 1982, and the M.S. and Ph.D. degrees in computer science and technology from Tsinghua University in 1984 and Hunan University in 2001, respectively. He has served as the Dean of the School of Information Science and Engineering, Central South University, where he is currently a Professor. Until now, he has published more than 100 papers in journals. His research focus is on computer graphics, image processing, and pattern recognition.

BIN XIE received the B.S. degree in electronic information engineering and the Ph.D. degree in information and communication engineering from Zhejiang University, China, in 2003 and 2008, respectively. He is currently an Associate Professor with the School of Information Science and Engineering, Central South University, China. His main research interests include medical image processing, machine learning, and robotics.